Theor Chem Acc (2004) 111:255–263
DOI 10.1007/s00214-003-0531-6

Theoretical
Chemistry Accounts

Regular article

Tailoring approach for exploring electron densities and electrostatic potentials of molecular crystals

K. Babu[1], **V. Ganesh**[1], **Shridhar R. Gadre**[1], **Nour E. Ghermani**[2]

[1] Department of Chemistry, University of Pune, 411 007, Pune, India
[2] Laboratoire de Physique Pharmaceutique UMR CNRS 8612, Faculté de Pharmacie 5, Université Paris XI, Rue Jean-Baptiste Clément, 92296, Châtenay-Malabry Cedex, France

Received: 16 January 2003 / Accepted: 30 April 2003 / Published online: 27 January 2004

Abstract. Experimental and theoretical studies of electron densities and the corresponding derived entities such as electrostatic potentials have been the primary means of understanding the chemical nature and electronic properties of crystalline substances. Conventional crystal calculation methods such as the embedded cluster models are capable of performing calculations on small and medium-sized molecules, while periodic ab initio methods can treat crystals with up to 200 atoms per unit cell. A linear scaling method, viz. the molecular tailoring approach, has recently been developed for obtaining ab initio quality one-electron properties. In the present study, the molecular tailoring approach is employed to generate electron density, electrostatic potential and interaction density maps with the ibuprofen crystal as a test case. The interaction density and electrostatic potential maps produced in the present work succinctly bring out the actual crystalline environment around a given reference molecule by including the interactions with atoms in its neighborhood. The results obtained from the molecular tailoring approach may thus be expected to enhance our understanding of the environment in the crystalline material with reasonably small computational effort.

Keywords: Molecular crystals – Electron densities – Electrostatic potentials – Molecular tailoring approach

Introduction

Electron densities (EDs) and properties derived therefrom are of fundamental importance to the understanding of the chemical nature of atoms, molecules and clusters [1]. Experimental techniques for reliable determination of ED, electrostatic potential (ESP) and other derived properties have been prevalent for several decades [2]. Recent developments, accelerated by the use of synchrotron X-ray sources and area detection techniques using charged coupled devices have revolutionized this field. Consequently, experiments to measure high-quality EDs [3] and determination of other one-electron properties are now becoming routine. However, an accurate theoretical computation of these one-electron properties using rigorous ab initio techniques is routinely possible only for systems with fewer than 100 atoms. The powerful numerical techniques developed in the framework of molecular quantum chemistry cannot be directly employed to extended systems [4] owing to the nonlinear scaling [$\sim O(N^3)$] of the Hartree–Fock (HF) and density functional theory (DFT) methods. In addition, obtaining a meaningful result from the data collected by X-ray diffraction experiment requires inputs from ab initio calculations, particularly so in the case of noncentrosymmetric structures [2]. There have been numerous attempts to compute band structures and electronic properties of solids using specialized techniques. This section provides a brief account of these methods with indicative references to the literature followed by a preamble to the present work.

Recent advances in the periodic ab initio techniques [4] have been of great utility to computational chemists studying the chemistry of solids. Periodic ab initio calculations yield crystal orbitals which reflect the translational symmetry of the crystal lattice. The obvious choice of plane waves as periodic functions is countered by the fact that even for systems with medium-sized asymmetric units, millions of plane waves are required. This makes the computations using plane waves a formidable task as the size of the unit cell increases. Alternatively, crystal ab initio programs have been developed that employ Bloch functions as molecular orbitals. Bloch functions are linear combinations of atomic orbitals which, in turn,

Contribution to the Jacopo Tomasi Honorary Issue

Correspondence to: Shridhar R. Gadre
e-mail: gadre@chem.unipune.ernet.in

are constructed from Gaussian functions. Methods that use a combination of plane waves (for electron-rich regions) and Bloch functions (for regions with sparse ED) are also gaining popularity.

The periodic ab initio methods have extended the scope of the "first principles" methods to systems containing up to 200 atoms per unit cell [5, 6]; however, the calculations become expensive as the number of atoms per unit cell increases. In addition, realistic modeling of crystal defects and inclusion complexes is rather difficult with the periodic ab initio methods, since such problems increase the asymmetry in periodic systems. Hence, there is continued interest in the theoretical investigation of crystals and other solids using embedded cluster models and supercell approaches [5, 7, 8, 9, 10, 11, 12, 13, 14]. In addition to the low computational cost, these methods have the advantage of providing a common platform for comparing the properties of molecules in a crystal to that of an isolated molecule. The embedded cluster methods treat quantum mechanically a very small part of the crystal which is embedded in an environment of potentials arrived through the Green function technique [15], DFT, or pseudopotential theory. This partition is conceptually similar to the recently popularized quantum mechanical (QM)/molecular mechanics (MM) methods. However, the computation of the Madelung contribution due to the embedding potential is still cumbersome except for simple ionic crystals [10, 11].

There are several variations of embedded potential techniques reported in the literature [5, 7, 8, 9, 10, 11, 12, 13, 14]. For example, Stefanovich and Truong [12] have developed a simple embedding scheme [12, 14] termed the surface charge representation of the electrostatic embedding potential method based on Gauss' law. In this model, the central cluster is treated at an appropriate QM level, while the immediate environment is represented by lattice charges and the potential due to the rest of the crystal is mimicked by a large number of discrete charges on the Gauss surface enclosing the central cluster. Ferenczy et al. [5] have devised a QM/MM-type model based on the self-consistent Madelung potential approach [16]. The central molecular region in this approach is treated at a semiempirical level. From these calculations, reliable estimates of the heats of sublimation have been obtained. Recently, Brändle et al. [6] have followed the deprotonation reaction of acidic sites of zeolite by ammonia, using periodic HF (PHF) and a combined QM/interatomic potential method reported in the literature [17]. This study also depicts the molecular ESP (MESP) plots at both these levels for ascertaining the most acidic site in the zeolite cage. The combined QM/interatomic potential model adopted by Brändle et al. [6] is seen to produce MESP plots qualitatively similar to their PHF counterparts. This work also highlights the inability of periodic ab initio methods to perform calculations on systems with a large number of basis functions per unit cell. In addition, it is stipulated that having a larger basis set is crucial, rather than allowing geometrical relaxation of the complex, for reliable prediction of interaction energies of the complex.

Other emerging alternatives to the periodic ab initio methods are the localized orbital methods and other linear-scaling methods. Shukla et al. [18] have used a Wannier-function-based HF method to investigate *trans*-polyacetylene. The geometry and energetics obtained from the calculation have been compared with the corresponding PHF results generated by the CRYSTAL [19] program. Bowler and Gillan [20] have gainfully employed the density matrix (DM) minimization method integrated with the McWeeny [21] purification scheme to perform quantum-embedded cluster calculations on defect sites created by substituting Ge in three types of Si clusters. This method divides the system into two regions: the first region contains the defect site and atoms in the immediate vicinity, while the rest of the cluster forms the second region. The DM elements in the second region are constrained to the values in the perfect crystal environment.

The molecular tailoring approach (MTA), a divide-and-conquer (DC)-type method was employed earlier by Gadre et al. [22] to compute one-electron properties of large molecules. The molecular ED (MED) and the MESP computed using the MTA were reported to be accurate to within 2% of the actual ab initio counterparts. Calculations have been reported [23] on a few test systems, including a silicious zeolite, containing up to 500 atoms. This approach also yields total electronic energies with reasonable accuracy. Huang et al. [24] have discussed quantum crystallography, employing their DC-type algorithm to study ED and difference density for a cyclic hexapeptide and an antibiotic, zervamicin, using the geometries from crystallographic data. This study hints at the direct applicability of linear scaling methods to crystals. Another DC-type model, viz. the transferable fragment ESP, was formulated by Zhong et al. [25] to obtain the ESP of large proteins from atom-based and fragment-based ESPs, similar to the MED Lego assembler (MEDLA) approach due to Mezey [26].[1] In this method, a set of unique atom or fragment (functional groups) types are identified from the target molecule and equivalent fragments are picked from a previously studied parent molecule. The target molecule is rebuilt from the picked atomic or molecular fragments (optimized individually) by a least-squares fit to the coordinates. The ESP of the target molecule is obtained as a superimposition of the atomic/molecular fragment ESPs. A larger error was observed when molecular fragments were used. This was attributed to the adjustment of atomic positions resulting from optimization of the fragments.

The cluster crystal orbital method put forward by Pelikán et al. [28] combines the advantages of the cluster

[1] A recent work reporting computation of MESPs of large molecules came to our attention while communicating the present work [27]

models and the crystal orbital methods. The errors in the cluster models due to the boundary effect and those in the crystal orbital methods due to an inadequate basis are eliminated. This is a generalization of the cyclic-cluster model formulated by Miró et al. [29]. This method enables one to perform periodic calculations using finite clusters that are computationally less expensive, at the same time maintaining reasonable accuracy. In their recent discussions on the topological analysis of the experimental and theoretical (PHF) EDs, Volkov et al. [30, 31] mention the ambiguities in the electronic properties derived from aspherical atom multipole refinements. It is pointed out that the results obtained from such calculations largely depend on the multipole model used [32]. Partitioning based on Bader's [33] atoms-in-molecule (AIM) approach has been suggested to overcome the inconsistency with the results from multipole refinements. However, the expense of the AIM-based atomic contributions to the charge and electrostatic moments has been noted. Further, the multipole refinement of theoretical structure factors introduces a bias in the topological properties of the charge density at the bond critical points, which is also manifested in the AIM-based results. This study [31] also provides an elaborate comparison of the MED topography of an isolated molecule with that obtained from the calculations which include ghost orbitals on surrounding molecules and for the crystal lattice using PHF. An extensive comparison of electronic properties, such as charge density, dipole moment, ESP and electric field gradient, of L-asparagine monohydrate derived from X-ray diffraction data with those obtained from theoretical calculations on isolated molecules within the HF and DFT formulations has been reported by Arnold et al. [34].

Spackman and Byrom [35] have discussed various schemes used to partition EDs of crystals into molecular components, in line with the AIM approach. The schemes of interest are the Hirshfeld surface (HS) and the extension of AIM, where molecular regions are formed by the union of atomic basins. Any electronic property obtained by integrating within these regions accounts for the property of the molecule in the crystal. The HS scheme provides an inexpensive way to compute electronic properties. McKinnon et al. [36] later employed the HS scheme to understand the interactions between molecules, using the comparison of naphthalene and terephthalic acid as a test case. The comparison brings out succinct differences in the interactions in crystals of these compounds. The HS scheme qualitatively shows the C–H$\cdots\pi$ interaction in naphthalene to be stronger than that in terephthalic acid, a feature which is reportedly not displayed by the corresponding isodensity surface and MESP textured van der Waals surface.

It may be pointed out that the emphasis of the aforementioned theoretical methods is on obtaining the band gaps, charge density distributions and bulk properties of crystals and polymeric materials. To the best of our knowledge, MESP computation of molecular crystals is rather scarce in the literature. In comparison to the ED distributions, the MESP plots are rich with topographical features providing significant information on the nature of bonding as well as the local electronic nature within the molecule [37]. In the present study, the electronic properties of the ibuprofen crystal were computed with a fully QM representation of the central region as well as the environment using the MTA. Ibuprofen is of immense medicinal value owing to its analgesic, antipyretic and anti-inflammatory properties. The interest in the present study was generated owing to a recent work by Bouhmaida et al. [38] which reports experimental determination of the MESP and presents the corresponding gradient paths.

Computational details

The methodology of the MTA is briefly outlined here. A detailed description of it can be found elsewhere [22, 23, 39]. As mentioned earlier, MTA is a linear-scaling ab initio method wherein the DM at the HF, DFT or post-HF levels of theory for a large molecular system (in a given fixed geometry) may be obtained by performing ab initio calculations on the appropriately formed smaller fragments of the parent system. It involves the following steps:

1. Break the parent system into a number of medium-sized (around 40 atoms) overlapping fragments.
2. Perform ab initio calculations at appropriate levels of theory on these fragmented molecular systems to obtain the respective single particle DMs.
3. Construct the DM of the supermolecule/cluster as a union of suitably selected elements from the DMs of the fragments.
4. Employ this super-DM for computation of electronic properties and energies.

The scissoring of the parent molecule into overlapping fragments and synthesizing the super-DM from the fragment DMs are crucial steps that directly influence the quality of the results.

The fragmentation process was carried out through elaborate programs written in FORTRAN 90 [23] and C++ [39]. It is necessary to follow certain "rules" when the fragments are being made. Weak bonds and C–C single bonds are preferentially cut over the olefinic, heteroatomic or other sensitive bonds. Aromatic rings and functional groups are kept intact in at least one of the fragments. The factors that govern the quality of the resulting DM are the size of the fragments and the extent of overlap between them. A comparison of the size and depth statistics provides information about the quality of the fragmentation scheme and helps to do a priori sampling of several (different sizes and overlap lengths) fragmentation schemes. The fragments are created by two different strategies. A breadth-wise traversal algorithm [23], wherein fragments are produced by traversing simultaneously along all the branches of the molecular tree. The fragments are created towards the end of the tree and the process is carried out recursively till an exhaustive fragmentation results. In the second strategy [39], the fragments are generated by collecting atoms that fall within a small parallelepiped placed over the molecular space. The parallelepiped is moved around the molecular space, maintaining an overlap between various parallelepipeds until the space is partitioned exhaustively. A posteriori analysis of the fragments so collected is carried out and the fragments are trimmed, merged or grown to adjust the fragment sizes and to correct for the errors arising out of cutting sensitive bonds and regions. The whole process from fragmenting the parent molecule to obtaining the super-DM is carried out in an automated manner, after sampling various fragmentation schemes.

The super-DM may be further improved by subjecting it to the McWeeny [21] purification scheme. It has been pointed by Chal-

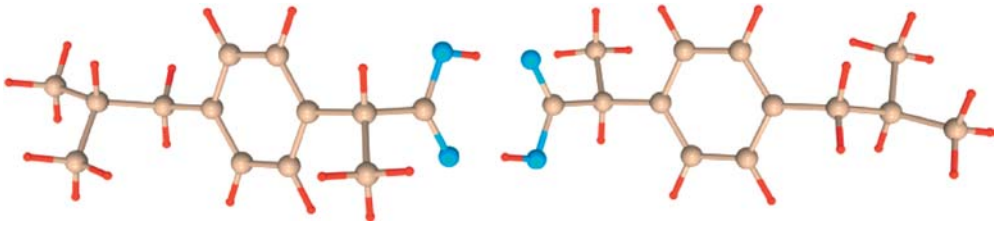

Fig. 1. Dimeric unit of the ibuprofen molecule

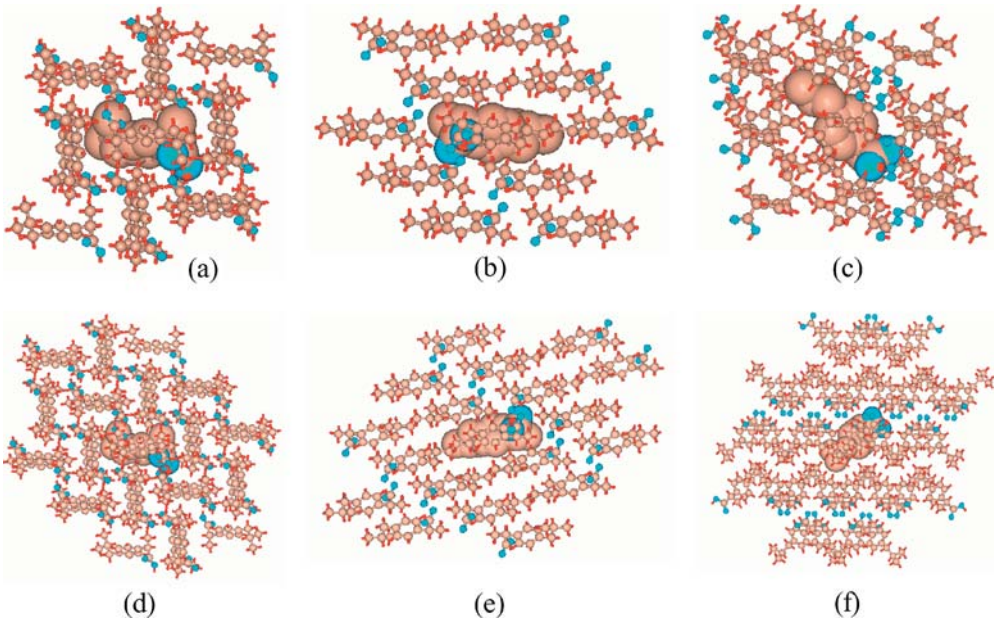

Fig. 2. Cluster 1 (*top*) and cluster 2 (*bottom*) consisting of 21 and 57 ibuprofen molecules, respectively, oriented along the 100 (**a**, **d**), 010 (**b**, **e**) and 001 (**c**, **f**) crystal faces. The central molecule is shown as a van der Waals surface

lacombe [40] that for a nonorthogonal basis this scheme can be written as

$$\mathbf{P}' = 3\mathbf{PSP} - 2\mathbf{PSPSP}.$$

Here, **P** is the guess DM of parent molecule and **P′** is the improved DM, which is more idempotent than **P**. Employing this procedure, our earlier studies (unpublished) have shown that the total electronic energy of the system can be obtained correctly by up to two decimal places without performing a single self-consistent-field (SCF) iteration for organic molecules containing up to 200 first-row/hydrogen atoms.

The self-consistent-field molecular orbital calculations on the fragments were carried out using the public domain program GAMESS [41]. All the calculations were carried out at the HF/6-31G(d,p) level of theory, unless specified otherwise. The MED, the MESP and the topography of the MESP were evaluated using the electronic property computation program UNIPROP [42][2]. All the graphic depictions in this article were produced using the visualization package UNIVIS-2000 [43].

Results and discussion

Clusters of two different sizes comprising 21 and 57 ibuprofen molecules, respectively,were built from the crystallographic data [38]. The clusters generated include all the molecules that have at least 25% of their atoms within a radius R_{cut} (9 and 11 Å for cluster 1 and cluster 2, respectively) from the central molecule. This provides a reasonably good mimic of an appropriate crystalline environment for the central molecule around which the electronic properties are computed. A dimer formed from two ibuprofen molecules is shown in Fig. 1; two hydrogen bonds due to carboxylic acid groups can be clearly seen. Clusters (1 and 2) oriented along the three crystallographic axes are displayed in Fig. 2. The central (core) molecule is shown as a van der Waals surface, while rest of the molecules in the cluster are displayed as a stick model. Although the core molecule in cluster 1 is mostly surrounded in all directions by other molecules, it is open in certain regions (Fig. 2b), omitting some weak interactions with the environment. This necessitated building a second, larger cluster containing 57 molecules. In addition, for the case of cluster 2, there is sufficient buffer to provide a realistic crystalline environment to the core molecule. Both clusters were fragmented via several different schemes and one scheme for each was chosen after a priori quantification [23] of the nature of the fragments. The fragmentation schemes chosen contain 78 and 237 fragments, respectively, for cluster 1 and cluster 2. The corresponding average sizes of the fragments turn out to

[2] Package UNIPROP can evaluate ab initio electronic properties such as the MESP, the MED, the Laplacian of the MED, the electron momentum density, the topography of all the properties, the internal electric field, and electronic moments up to third order

be 34.5 and 51.1 atoms. The fragment molecules so obtained were subjected to molecular orbital calculation at the HF/6-31G(d,p) level of theory. The DM of the whole cluster was then synthesized [22, 23] from the molecular DMs of the fragment.

In order to assess the quality of the DM synthesized, it was felt worthwhile to compare it with the actual DM (here and elsewhere in the text, actual refers to the results obtained by performing an ab initio level calculation on the cluster as a whole). However, the 6-31G(d,p) basis set entails 6,615 contracted Gaussian functions for cluster 1: a formidable computational task even at the HF level of theory. Hence for the sake of comparison, the actual and synthesized DMs were computed (all the computations reported here were carried out at the HF level of theory) for cluster 1 using the minimal basis set (STO-3G). The time taken to obtain the actual DM was 78 h when employing a parallel version of GAMESS on a cluster of four Pentium 4 computers (at 1.7-GHz clock speed and with 256 MB random access memory) running on GNU/Linux. On the other hand, it took only about 1 h to get the synthesized DM. The times taken to obtain the synthesized DMs at the HF/6-31G(d,p) level for cluster 1 and cluster 2 were 50 and 180 h, respectively (on a single Pentium 4 computer at 1.5-GHz with 512 MB random access memory). It is anticipated that the corresponding computer time for generating the respective actual DM would be of the order of several weeks even if higher hardware requirements (such as memory) are met. A pictorial comparison of the actual and synthesized DMs at the HF/STO-3G level is shown in Fig. 3. Each DM element is represented with pixels of appropriate color codes. The atom (and hence the contraction) indices are sorted so as to present the bonded atoms in sequence. As a result, 21 small triangles along the diagonal can be noticed (Fig. 3a, b), which represent 21 molecules with strong intramolecular bonds within them. Green patches with embedded brown in the off-diagonal region (Fig. 3a) are the cross-molecule terms arising owing to weak intermolecular interactions. The synthesized DM faithfully produces the numerically significant values (yellow to red), while the numerically insignificant values (green), largely located in the intermolecular region of the actual DM, are partly absent. It should be emphasized here that the missing elements in the synthesized DM are of the order 10^{-6}–10^{-5} and hence no significant loss in the quality of one-electron properties computed using the synthesized DM is anticipated.

The 3D graph in Fig. 4 brings out the quantitative difference between the actual and synthesized DMs. It presents a comparison of the DMs in various numerical ranges. From Fig. 4, it is evident again that numerically significant DM elements ($|P_{ij}| > 0.1$) have very small error (much less than 5.0%), while the last range of values ($0.1 > |P_{ij}| > 0.01$) also lie predominantly in the low-error region (less than 5.0%). It may be noted here that the logarithmic scale was used to represent the number of elements falling in a given range of errors (y-axis).

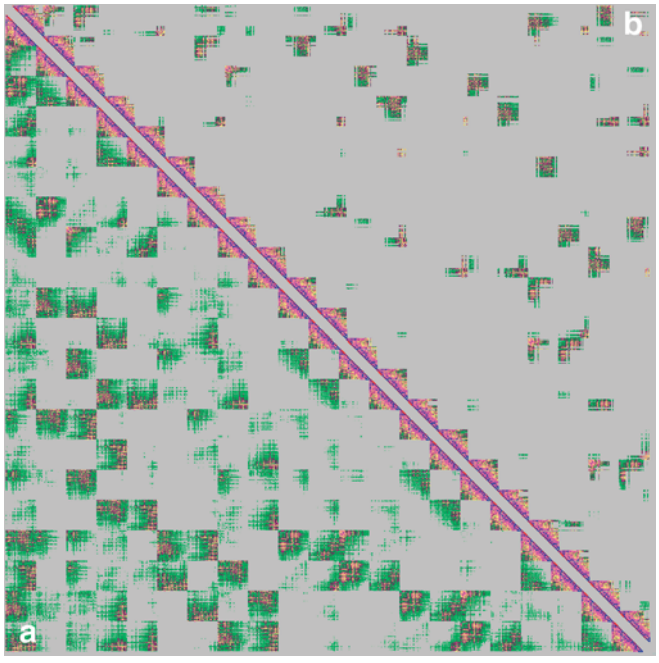

Fig. 3. Comparison of the elements of **a** actual and **b** synthesized density matrixes (*DMs*) for cluster 1 of the ibuprofen molecule, computed at the HF/STO-3G level of theory. For the purpose of clarity only the lower triangular matrix of the actual DM and the upper triangular matrix of the corresponding synthesized DM separated by a *gray band* along the diagonal are shown. Color codes are used to denote the numerical range of the DM elements. (*Red* greater than 10^{-1}, *blue* 10^{-2}–10^{-1}, *magenta* 10^{-3}–10^{-2}, *yellow* 10^{-4}–10^{-3}, *brown* 10^{-5}–10^{-4}, *green* 10^{-6}–10^{-5}). DM elements that are numerically less than 10^{-6} are not displayed. See text for further description

Although such a comparison is not feasible when the 6-31G(d,p) basis set is used, Tr(**PS**) provides a measure of the overall quality of the DM. For cluster 1, Tr(**PS**) at the HF/6-31G(d,p) level turns out to be 2,351.962, i.e., an error of around 0.04 electrons. The error for cluster 2 (57 molecules) at the same level of theory is just 0.005 electrons (of 6,384 electrons). All these analyses ascertain that the synthesized DMs mimic their actual counterparts quite faithfully. Nevertheless, the synthesized DMs were uniformly scaled to correct the minor error in Tr(**PS**). The scaled DMs thus obtained were employed to calculate one-electron properties of the ibuprofen molecule in a crystal.

It was shown in our earlier studies [22, 23] that MEDs are produced fairly accurately even with smaller fragments. Though the MED is an extensively studied scalar field, it does not directly reveal any meaningful information about the molecular interactions in its unmodified form. However, the interaction density (ID) maps, defined as the difference between the MED and the sum of atomic densities, viz. $\rho_{\mathrm{ID}}(r) = \rho_{\mathrm{mol}}(r) - \sum_{\mathrm{atom}} \rho_{\mathrm{atom}}(r)$, are known [1] to be of more utility than the MED itself. The ID plots clearly bring out regions of electron depletions and concentrations due to the covalent/ionic bond formation. Analogously, the molecular ID (MID), defined as the difference in density of the supermolecule

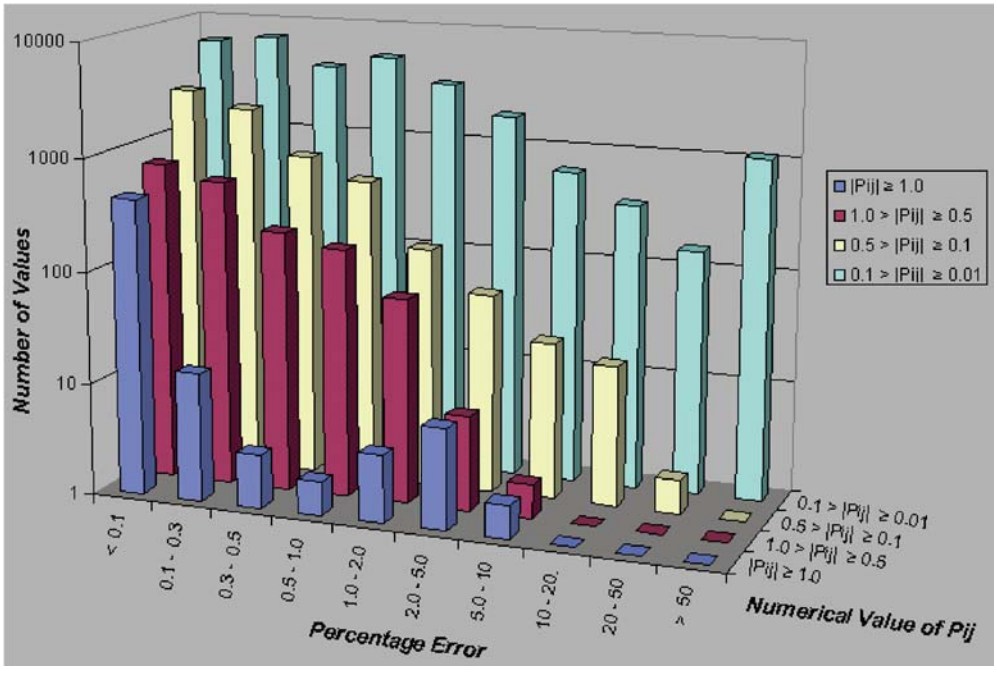

Fig. 4. Variation of the synthesized DM compared to the actual one for the HF/STO-3G calculation on the ibuprofen molecule. See text for discussion

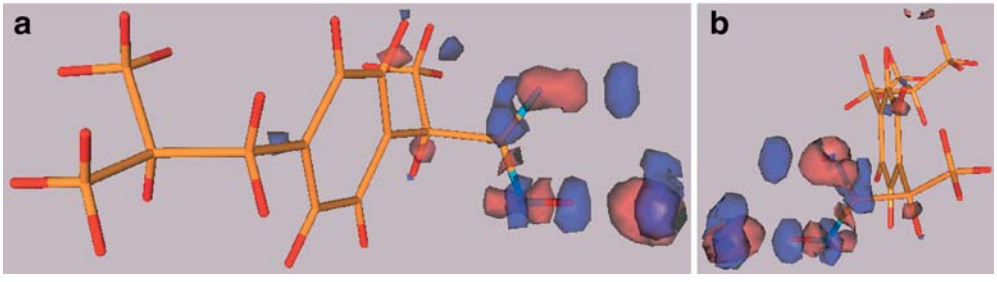

Fig. 5a,b. Difference density, $\Delta\rho$, plots for the ibuprofen crystal computed [HF/6-31G(d,p)] using the synthesized DM of cluster 1. **a** and **b** depict isosurfaces of values 0.003 au (*red*) and –0.003 au (*blue*) in two different views. See text for a detailed discussion

and the sum of densities of individual molecules, have also been reported [1] in the literature for investigating interactions between molecules. In the present study, MID plots were obtained for both clusters studied here with a view to bring out the specific interactions existing in the region representing the crystal lattice. Figs. 5a and 5b depict MID isosurfaces of values −0.003 and 0.003 au (the convention of blue indicating a negative-valued function and red the positive-valued one has been used throughout in this article). Since the dimer forms the basic building block of the crystal and no other strong hydrogen bonds exist, the primary MID features are visible only in the dimeric carboxylic acid groups. Figure. 5a and b clearly brings out the charge transfer from the acidic hydrogen to the carbonyl oxygen of its dimeric partner. This charge transfer is compensated by the electron flow along the covalent bond within the molecule, resulting in alternating positive-valued (red) and negative-valued (blue) MID isosurfaces forming a ring-like structure. Major electronic rearrangements occur within the dimer unit. Other small surfaces near the isobutyl group and the ortho position (with respect to the carboxylic group) in the benzene ring indicate feeble interactions with neighboring molecules. These features are more clearly conveyed by the $\rho_{\mathrm{ID}}^{\mathrm{dimer}}(\mathbf{r})$ (Fig. 6), which is defined as the difference between $\rho(\mathbf{r})$ for cluster 2 and that of the dimer, viz. $\rho_{\mathrm{ID}}^{\mathrm{dimer}}(\mathbf{r}) = \rho_{\mathrm{cluster\ 2}}(\mathbf{r}) - \rho_{\mathrm{dimer}}(\mathbf{r})$.

Here, the textured van der Waals surface (scaled by a factor of 0.9) was employed to bring out these density differences. Fig. 6 reveals that there is a gain in ED on either side of the phenyl carbon connected to the isobutyl group and on the carbonyl carbon, while there is a depletion of ED along two phenyl hydrogen atoms and the hydroxyl oxygen.

The scalar field of the MESP is known to bring out electron localization features very vividly and has become a popular tool for studying weak intermolecular interactions [37]; hence, the MESP was computed for the isolated molecule, the isolated dimer, cluster 1 and cluster 2 over a parallelepiped constructed around the central molecule. A comparison of the MESP textured on the van der Waals surface is shown in Fig. 7. The pictures display the MESP due to an isolated ibuprofen molecule, an isolated ibuprofen dimer, cluster 1 and cluster 2 textured on the central molecule. In Fig. 7a, the highly negative MESP region due to the carbonyl and hydroxyl oxygen atoms together with the weakly nega-

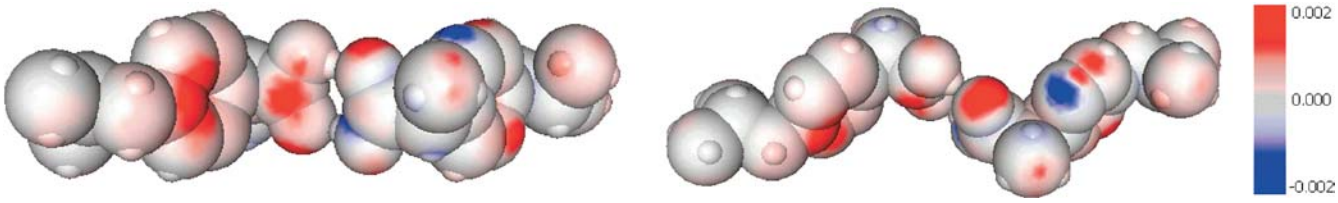

Fig. 6. Difference density, $\Delta\rho_{dimer}$ ($\rho_{cluster\ 2}-\rho_{dimer}$), textured on the scaled (0.9) van der Waals surface of the ibuprofen dimer. See text for details

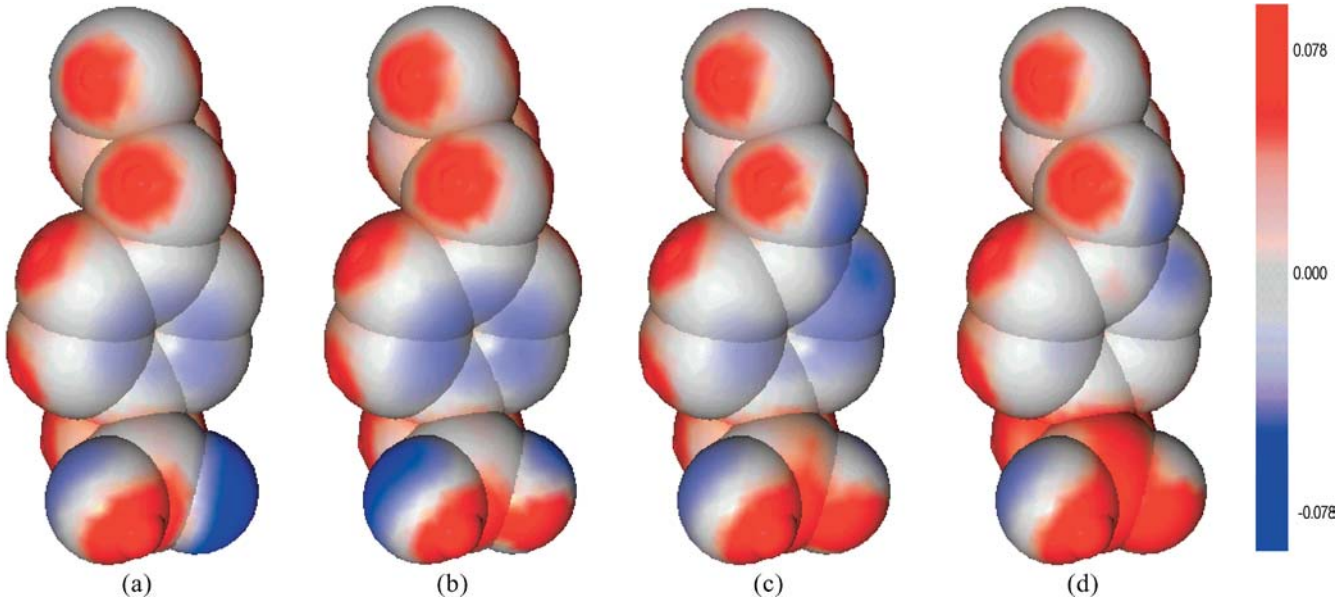

Fig. 7. Molecular electrostatic potential [HF/6-31G(d,p)] due to **a** an isolated monomer, **b** an isolated dimer, **c** cluster 1 and **d** cluster 2 of the ibuprofen molecule textured on the van der Waals surface of the core molecule. See text for further details

tive region over the phenyl ring of the ibuprofen molecule are shown in blue. The red regions describe the hydrogen atoms. The phenyl ring shows an overall electron-withdrawing effect due to the presence of carbonyl group. The negative region surrounding the carbonyl group is conspicuous by its absence in the textured MESP plot (Fig. 7c) of cluster 1. The region over the benzene ring is more negative in comparison to Fig. 7a owing to the lesser electron-withdrawing effect of the carbonyl group as well as to the contribution from the crystalline environment. The C–H···O interactions of the reference molecule with the oxygen atoms in the vicinity (viz. 2.6–2.8 Å) seem to be responsible for these features. Similar features are noticed in Fig. 7d, which are somewhat less pronounced in nature. Since cluster 2 features the crystalline environment effect in a more faithful way, Fig. 7d is expected to be a better representative picture of an ibuprofen molecule in a crystalline environment.

The MESP topography can be characterized in terms of the position and the nature of its critical points (CPs). A suitably modified version of the package UNIPROP [42] was used for the identification and characterization of MESP CPs of the isolated ibuprofen dimer. A comparison with the corresponding features obtained from cluster 1 is shown in Table 1 (The atomic coordinates of cluster 1 and cluster 2 are available from the authors on request). The negative-valued minima near the carbonyl and hydroxyl oxygen atoms of the acid group bear the MESP values of –0.0796 and –0.0620 au, respectively, in the isolated dimer. Owing to weak attractive interactions with the neighboring molecules, they attain relatively less pronounced values (negative) viz. –0.0598 and –0.0530 au. In contrast, one of the MESP minima over the benzene ring (–0.0281 au) is seen to become more pronounced (–0.0410 au) and is also displaced by around 1 au from its counterpart in the isolated dimer, while the minima on the other side of the ring is only slightly altered in its value and position. This may be attributed to the C–H···O interaction with the oxygen atom in the vicinity of the core molecule (Fig. 7). The two phenyl MESP minima in the cluster are located at an approximate distance of 1.74 Å from the nearest ring carbon compared to the dimer ones, which are typically 1.87 Å away. This observation is in good qualitative agreement with the results reported by Bouhmaida et al. [38]; however, in quantitative terms, the CPs reported by them are much closer to the phenyl ring. The lone-pair MESP minima in the ibuprofen crystal are reported by Bouhmaida et al. [38] to be at a distance of 1.1 Å from

Table 1. Cartesian coordinates and values of the molecular electrostatic potential [HF/6-31G(d,p)] at the (3, +3) critical points computed for an isolated ibuprofen dimer and the core molecule in cluster 1. All the values are in atomic units. See text for details. (The atomic coordinates of cluster 1 are available from the authors on request)

Isolated dimer				Cluster 1			
x	y	z	$V(\mathbf{r})$	x	y	z	$V(\mathbf{r})$
3.738	−5.345	5.742	−0.0796	3.822	−5.306	5.858	−0.0598
11.076	−9.592	5.512	−0.0620	11.082	−9.466	6.235	−0.0530
9.660	−0.470	0.661	−0.0281	8.785	−0.001	0.180	−0.0410
9.700	−7.394	−0.605	−0.0332	9.932	−7.258	−0.233	−0.0320

the oxygen nucleus. The corresponding average distance obtained in the present work is 1.2 Å. However, the respective MESP values differ substantially.

The dimer of the ibuprofen molecule (Fig. 1) was employed as a basic unit in the studies of the MID as well as the MESP. The positive and negative regions of the MID as well as the enhancement of the MESP features may be attributed to weak intermolecular interactions such as C−H···O or C−H···π-type present in the cluster. Thus, the ibuprofen dimer in the cluster shows subtle but definite differences from the corresponding isolated dimer.

Concluding remarks

The purpose of the present work is to derive reliable one-electron properties of large molecules, for which a direct HF/DFT or higher-level calculation is impractical, using the currently available computing power. For this purpose, a DC-type algorithm viz. MTA, was developed in our laboratory and was applied earlier to large single molecules such as a zeolite and a polypeptide. The current study aims at extending this approach for exploring molecular crystals. As an example, the interactions in a crystal of weakly interacting ibuprofen molecules were investigated employing the MTA. Appropriately defined clusters of 21 and 57 molecules were cut out for mimicking the ibuprofen crystal. The DM synthesized from the corresponding fragment counterparts incorporate major strong as well as weak interatomic interactions. The DM synthesized at the HF/STO-3G level is seen to match reasonably with the corresponding actual one. It is noteworthy that the synthesized DM was computed in a fraction of the time required for computing the actual DM. Needless to say, the corresponding factor at the HF/6-31G(d,p) level would be much higher assuming that such a calculation is at all possible.

The typical error in the ED is seen to be less than 0.1% at points in the vicinity of the molecule. At the same time, it is observed that the error in the MESP is somewhat larger owing to the positive and negative contributions that make up the scalar field. However, the error in the MESP calculated at the HF/STO-3G level does not exceed 5%. In particular, the region near strongly negative-valued MESP minima and saddle points are seen to be reproduced quite well, the typical error being 2%. Though the benchmark was performed at the HF level, the same technique is applicable for calculations with better levels of theory, such as DFT or second-order Møller–Plesset (MP2).

The present approach employs the geometry derived from X-ray diffraction experiments. Secondly, no further approximations such as multipole refinement, etc., are made. Thus it may be expected that the ED and allied one-electron properties obtained in the central region of a chosen cluster are of reliable quality. A recent study by Bouhmaida et al. [38] has presented a picture of the MESP of the ibuprofen molecule in a crystal employing Bader's AIM approach. The present work has exhibited some features in qualitative agreement with their results. It would hence be worthwhile to compare and contrast our results in detail with those obtained [38] from experimental data. It may be hoped that the ED thus derived employing the MTA at a high level of theory (DFT/MP2) and basis set can be used as an input for crystallographic studies. Further, the MESP distribution due to the cluster is expected to provide valuable guidelines for the investigation with interacting molecules on the surfaces, inclusion complexes etc.

Acknowledgements. The authors are thankful to the Centre for Development of Advanced Computing (C-DAC), Pune, India, for computational facilities. V.G. and K.B. acknowledge support from the C-DAC and the Council of Scientific and Industrial Research, New Delhi, India, respectively. We are grateful to Claude Lecomte (University Henry Poincaré, Nancy, France) for initiating a discussion on ED distributions of molecular crystals.

References

1. (a) Coppens P (1997) X-ray charge densities and chemical bonding. Oxford University Press, Oxford; (b) Coppens P, Stevens ED (1997) In: Löwdin P-O (ed) Advances in quantum chemistry. Academic, New York, pp
2. Koritsanszky TS, Coppens P (2001) Chem Rev 101:1583
3. (a) Boese R, Blaeser D, Heinemann O, Abramov Y, Tsirelson V, Blaha P, Schwarz K (1999) J Phys Chem A 103,:6209; (b) Ivanov YV, Zhurova EA, Zhurov VV, Tanaka K, Tsirelson VG (1999) Acta Crystallogr Sect B 55:923
4. Pisani C, Dovesi R, Roetti C (1988) Hartree–Fock ab initio treatment of crystalline systems. Springer lecture notes in chemistry 48. Springer, Berlin, Heidelberg New York
5. Ferenczy GG, Csonka GI, Naray-Szabo G, Ángyán JG (1998) J Comput Chem 19:38
6. Brändle M, Sauer J, Dovesi R, Harrison NM (1998) J Chem Phys 109:10379
7. Grimes RW, Catlow CRA, Shluger AL (eds) (1992) Quantum mechanical cluster calculations in solid-state studies. World Scientific, Singapore
8. Pacchioni G, Bagus PS, Parmigiani F (eds) (1992) Cluster models for surface and bulk phenomena. Plenum, New York
9. Kaplan TA, Mahanti SD (eds) (1995) Electronic properties of solids using cluster methods. Plenum, New York
10. Jaffe JE, Hess AC (1996) J Chem Phys 105:10983
11. Saunders VR, Freyria-Fava C, Dovesi R, Salasco L, Roetti C (1992) Mol Phys 77:629
12. Stefanovich EV, Truong TN (1998) J Phys Chem B 102:3018, and references therein

13. Gutdeutsch U, Birkenheuer U, Krüger S, Rösch N (1997) J Chem Phys 106:6020
14. Johnson MA, Troung TN (1999) J Phys Chem B 103:9392
15. Pisani C, Birkenheuer U (1995) Int J Quantum Chem Quantum Chem Symp 29:221
16. (a) Ángyán JG, Silvi B (1987) J Chem Phys 86:6957; (b) Ángyán JG, Silvi B (1990) In: RivailJ-L (eds) Modelling of molecular structures and properties. Elsevier, Amsterdam, pp
17. Eichler U, Kölmel CM, Sauer J (1996) J Comput Chem 18:463
18. Shukla A, Dolg M, Stoll H (1998) Phys Rev B 58:4325
19. Wesolowski TA, Chermette H, Webber J (1996) J Chem Phys 105:9182
20. Bowler DR, Gillan MJ (2002) Chem Phys Lett 335:306
21. McWeeny R (1962) Rev Mod Phys 126:1028
22. Gadre SR, Shirsat RN, Limaye AC (1994) J Phys Chem 98:9165
23. Babu K, Gadre SR (2003) J Comput Chem 24:484
24. Huang L, Massa L, Karle J (2001) IBM J Res Dev 45:410
25. Zhong S, Dadarlat VM, Glaeser RM, Head-Gordon T, Downing KH (2001) Acta Crystallogr Sect A 58:162
26. Mezey PG (1995) J Math Chem 18:141
27. Exner TE, Mezey PG (2002) J Phys Chem A 106:11791
28. Pelikán P, Zajac A, Banacký P, Noga J, Biskupic S, Svrcek M http://www.fch.vutbr.cz/mol/sbornik/pelikan/
29. Miró J, Deák P, Ewels CP, Jones R (1997) J Phys Condens Matter 9:9555
30. Volkov A, Gatti C, Abramov Y, Coppens P (2000) Acta Crystallogr Sect A 56:252
31. Volkov A, Abramov Y, Coppens P, Gatti C (2000) Acta Crystallogr Sect A 56:332
32. Abramov YA, Volkov AV, Coppens P (1999) Chem Phys Lett 311:81
33. Bader RFW (1990) Atoms in molecules—a quantum theory. Oxford University Press, Oxford
34. Arnold WD, Sanders LK, McMahon MT, Volkov AV, Wu G, Coppens P, Wilson SR, Godbout N, Oldfield E (2000) J Am Chem Soc 122:4708
35. Spackman MA, Byrom PG (1997) Chem Phys Lett 267:215
36. McKinnon JJ, Mitchell AS, Spackman MA (1998) Chem Commun 2071
37. (a) Gadre SR, Shirsat RN (2000) Electrostatics of atoms and molecules. Universities Press, India; (b) Scrocco E, Tomasi J (1978) Adv Quantum Chem 11:116; (c) Pullman B (1990) Int J Quantum Chem Quantum Biol Symp 17:81
38. Bouhmaida N, Dutheil M, Ghermani NE, Becker P (2002) J Chem Phys 116:6196
39. Ganesh V, Kashid M (2002) MCS dissertation. Interdisciplinary School of Scientific Computing, University of Pune, India
40. Challacombe MJ (1999) Chem Phys 110:2332
41. (a) Granovsky A, http://classic.chem.msu.su/gran/gamess/index.html; (b) Schmidt MW, Baldridge KK, Boatz JA, Elbert ST, Gordon MS, Jensen JH, Koseki S, Matsunaga N, Nguyen KA, Su SJ, Windus TL, Dupuis M, Montgomery JA (1993) J Comput Chem 14:1347
42. Shirsat RN, Bapat SV, Gadre SR (1992) Chem Phys Lett 200:373
43. Limaye AC, Gadre SR (2001) Curr Sci (India) 80:1296